

# Sulfate reduction and sulfide oxidation in extremely steep salinity gradients formed by freshwater springs emerging into the Dead Sea

Stefan Häusler<sup>1</sup>, Miriam Weber<sup>1,2</sup>, Christian Siebert<sup>3</sup>, Moritz Holtappels<sup>1</sup>, Beatriz E. Noriega-Ortega<sup>4</sup>, Dirk De Beer<sup>1</sup> & Danny Ionescu<sup>1,5</sup>

<sup>1</sup>Max Planck Institute for Marine Microbiology, Bremen, Germany; <sup>2</sup>Elba Field Station, HYDRA Institute for Marine Sciences, Elba, Italy;

<sup>3</sup>Department of Catchment Hydrology, Helmholtz-Center for Environmental Research-UFZ, Halle/Saale, Germany; <sup>4</sup>ICBM-MPI Bridging Group for Marine Geochemistry, Oldenburg, Germany; and <sup>5</sup>Leibniz Institute for Freshwater Ecology and Inland Fisheries, IGB, Dep 3, Experimental Limnology, Stechlin, Germany

**Correspondence:** Danny Ionescu, Leibniz Institute for Freshwater Ecology and Inland Fisheries, IGB, Dep 3, Experimental Limnology, Alte Fischerhütte 2, OT Neuglobsow, 16775 Stechlin, Germany. Tel.: + 49 (0)3308 269969; fax: +49 (0)3308 269917; e-mail: ionescu@igb-berlin.de

Received 19 May 2014; revised 9 October 2014; accepted 19 October 2014. Final version published online 17 November 2014.

DOI: 10.1111/1574-6941.12449

Editor: Gary King

## Keywords

salinity fluctuation; halophilic sulfate reducers; isotopic fractionation; *Epsilonproteobacteria*.

## Introduction

The Dead Sea, located between Jordan, Israel and the Palestinian Authorities, is one of the most hypersaline lakes on our planet. It is the lowest exposed surface on earth [−427 m mean sea level (value correct to 2014)] and consists of a deep northern and a shallow southern basin. Since the middle of the 20th century the water budget of the Dead Sea has been negative due to the diversion of freshwater from its drainage basin and the use of the lake's brines for industrial salt production (Oren, 2010). As a result, over the last decades there has been a constant drop in the lake level of about 1 m year<sup>−1</sup> (Lensky *et al.*, 2005) and a continuous change of the physico-chemical properties of the water.

## Abstract

Abundant microbial mats, recently discovered in underwater freshwater springs in the hypersaline Dead Sea, are mostly dominated by sulfur-oxidizing bacteria. We investigated the source of sulfide and the activity of these communities. Isotopic analysis of sulfide and sulfate in the spring water showed a fractionation of 39–50‰ indicative of active sulfate reduction. Sulfate reduction rates (SRR) in the spring sediment (< 2.8 nmol cm<sup>−3</sup> day<sup>−1</sup>) are too low to account for the measured sulfide flux. Thus, sulfide from the springs, locally reduced salinity and O<sub>2</sub> from the Dead Sea water are responsible for the abundant microbial biomass around the springs. The springs flow is highly variable and accordingly the local salinities. We speculate that the development of microbial mats dominated by either Sulfurimonas/Sulfurovum-like or *Thiobacillus*/Acidithiobacillus-like sulfide-oxidizing bacteria, results from different mean salinities in the microenvironment of the mats. SRR of up to 10 nmol cm<sup>−3</sup> day<sup>−1</sup> detected in the Dead Sea sediment are surprisingly higher than in the less saline springs. While this shows the presence of an extremely halophilic sulfate-reducing bacteria community in the Dead Sea sediments, it also suggests that extensive salinity fluctuations limit these communities in the springs due to increased energetic demands for osmoregulation.

The salinity and density of the brine has increased, resulting in an overturn in 1979, ending a century long meromictic phase which was characterized by an anoxic, sulfidic bottom and an oxic surface water body (Steinhorn *et al.*, 1979). Nowadays, the lake is holomictic with a total dissolved salt (TDS) concentration of > 340 g L<sup>−1</sup>. Saturation of NaCl in the water column has led to continuous precipitation of halite. Thus, the more soluble Mg<sup>2+</sup> and Ca<sup>2+</sup> ions have become the dominant cations [about 2 and 0.5 M, respectively (in addition to 1.5 M Na<sup>+</sup>); Oren, 2010]. The extreme salinity and especially the high concentrations of divalent cations, which have a high chaotropic (destabilizing) effect on biological macromolecules (Oren, 2013), make the Dead Sea an extreme environment.

These harsh conditions are only tolerated by a few types of microorganisms, as reflected in the low microbial diversity. Generally, the microbial community of the Dead Sea ecosystem seems to be dominated by Archaea (Bodaker *et al.*, 2010). The only primary producer detected in the lake is the unicellular algae *Dunaliella* sp. (Oren, 2010). However, extensive blooms of the algae only develop during periods when the upper water layer of the lake becomes sufficiently diluted after severe rainfall and subsequent runoff events. Such bloom events were monitored in 1980 and 1992 and were followed by blooms of Archaea living on the exudates of the autotrophic algae (Oren & Shilo, 1982, 1985; Oren, 1983; Oren *et al.*, 1995). In addition to these microorganisms, several Archaea and Bacteria species, as well as protozoa and ciliates have been isolated from the water column and the sediments of the lake (Elazari-Volcani, 1943a, b, 1944; Oren, 2010). Sulfate-reducing bacteria (SRB) have never been isolated from the Dead Sea (Oren, 2010). However, at times when the lake was still permanently stratified, a difference of 35‰ in the  $\delta^{34}\text{S}$  value between dissolved sulfide and sulfate and the depletion in  $\delta^{34}\text{S}$  by 25–35‰ in iron sulfide in the sediment, indicated the presence of sulfate-reducing activity in the lake (Nissenbaum, 1975).

Recently, a large system of underwater freshwater springs emerging into the northern basin of the Dead Sea was discovered (Ionescu *et al.*, 2012). The water originates from the Upper Cretaceous Aquifers and flows through the Quaternary sediments of the Dead Sea and its precursors until it emerges along the shoreline at depths of 2–30 m into the lake. The discovered system is divided into a northern and a southern part. In the northern part the springs are located at the bottom of deep shafts (10–30 m), whereas in the southern part these shafts are absent and the water emerges either as jets from distinct outlets or as widespread slow seeps from the Dead Sea sediments. Based on 16S rRNA gene analysis and microscopic observations, it was concluded that these springs harbor an unusually high and diverse biomass of microorganisms compared with the surrounding Dead Sea. For instance, rocks and cobbles located in the jets of the southern system are covered with thick green and white biofilms mainly composed of phototrophic and chemolithotrophic sulfur-oxidizing bacteria (SOB). On the other hand, at seeping sites microbial mats are dominated by SOB belonging to the *Epsilonproteobacteria* (Ionescu *et al.*, 2012). In addition, sequences of SRB were detected in the spring sediments and the surrounding Dead Sea (Ionescu *et al.*, 2012).

The main reason for the high microbial biomass is probably the development of microenvironments of reduced salinity on surfaces exposed to spring water

discharge (Häusler *et al.*, 2014). In addition, the springs deliver organic matter (OM) and sulfide (Ionescu *et al.*, 2012), which could fuel the SRB and the SOB communities, respectively. Thus, the aim of this study was to investigate whether the sulfur-related microbial community suggested from the sequencing analysis is indeed active. Furthermore, we aim to elucidate whether the sulfide in the spring water is produced locally in the spring sediments, or most likely along the subsurface passage through the Quaternary sediments, rich in OM and sulfate minerals, by bacterial sulfate reduction. To answer these questions we used a polyphasic approach. First, we used the isotopic signature of coexisting sulfate and sulfide in the spring water to determine the source of sulfide. Secondly, we performed *in situ* microsensor measurements on two microbial mats to establish the activity of the SOB community. Thirdly, we used radiolabeling experiments to determine sulfate reduction rates (SRR) in the spring and the surrounding Dead Sea sediments. In combination with 16S rRNA gene sequences detected in the different microbial mats we furthermore speculate that differences in the community of SOB and SRB related sequences between distinct spring water outlets are a result of different spring water flow regimes leading to different mean salinities.

## Material and methods

### Sampling strategy

Samples were collected by SCUBA divers from the springs shown in Supporting Information Fig. S1. Sediment samples were collected in cores for measurements of sulfate reduction rate or in sterile 50-mL tubes for community analysis, as detailed below. Water was sampled by manually positioning a 40-m tube released from a boat, in the sediment of the spring as detailed in Ionescu *et al.* (2012). Sulfide,  $\text{O}_2$ , pH and redox potential microprofiles were measured *in situ* as detailed below.

### Analysis of water samples

Chemical analysis of the water samples was done as described by Ionescu *et al.* (2012). For isotopic measurements of sulfide, 6 mL of spring water was collected in Exetainers prefilled with 100  $\mu\text{L}$  of 20% zinc acetate (w/v) to fix S(-II) as  $\text{ZnS}$ . The contents of the vials were then filtered using a 0.2  $\mu\text{m}$  polycarbonate filter (Millipore). Subsequently, sulfate was precipitated as  $\text{BaSO}_4$  in the filtrate by acidification with 1 M HCl (to pH 3) following the addition of 150  $\mu\text{L}$  of 1.2 M  $\text{BaCl}_2$ . The precipitate was recovered on a separate 0.2- $\mu\text{m}$  polycarbonate filter. All filters were dried at 60 °C for at least 12 h.

Sulfur isotope measurements were performed by continuous flow isotope ratio mass spectrometry at the Geological Institute, ETH Zurich. Sulfur isotope data are reported in the standard  $\delta$ -notation relative to the Vienna-Canyon Diablo Troilite (V-CDT), i.e.  $\delta^{34}\text{S} = (R_{\text{sample}}/R_{\text{V-CDT}} - 1) \times 10^3\text{‰}$ . The system was calibrated using the international standards IAEA-S1 ( $\delta^{34}\text{S} = -0.3\text{‰}$ ), IAEA-S2 ( $\delta^{34}\text{S} = 22.7\text{‰}$ ), NBS123 ( $\delta^{34}\text{S} = 0.5\text{‰}$ ) for sulfide precipitates and for  $\text{S}^0$ ; the  $\text{S}^0$  analyses were controlled with the standard IAEA-S-4 (Soufre de Lacq;  $\delta^{34}\text{S} = 16.9\text{‰}$ ), IAEA-SO5 ( $\delta^{34}\text{S} = 0.5\text{‰}$ ), IAEA-SO6 ( $\delta^{34}\text{S} = -34.1\text{‰}$ ) and NBS127 ( $\delta^{34}\text{S} = 21.1\text{‰}$ ; Halas & Szaran, 2001) were used for  $\text{BaSO}_4$  precipitates. The analytical reproducibility of replicate measurements of standards is  $\pm 0.3\text{‰}$  ( $n = 319$ ).

In addition, for fingerprint analysis of dissolved OM, Dead Sea water (DSW) samples ( $n = 43$ ) were collected using Niskin entrapment bottles at different depths between 6 and 166 m along a transect from shore and up to 1000 m away. Samples were transferred directly into an acid-rinsed 1-L plastic bottle. Samples from the aquifers were collected from various wells ( $n = 19$ ). Thirty samples of underwater springs were analyzed.

### DOM extraction and sample preparation

DOM was extracted from the water samples ( $n = 46$ ) by solid phase extraction (SPE; Dittmar *et al.*, 2008) with the following modifications; samples were not filtered prior to DOM extraction and 1 L of sample was diluted 1 : 1 with ultrapure water. The samples were acidified to pH 2 with HCl analytical grade and run through Varian Bond Elut PPL resins by gravity.

### FT-ICR-MS data processing

Ultrahigh-resolution mass spectrometry via the Fourier transform ion-cyclotron resonance (FT-ICR-MS) technique was performed on a Bruker Solarix 15 Tesla FT-ICR-MS. Electrospray ionization was in negative mode and 500 scans were accumulated. Samples were injected at a flow rate of  $120 \mu\text{L h}^{-1}$  and the mass range analyzed was 180–2000  $m/z$ . Molecular formulae were assigned for all samples using data analysis software (Esi Compass 1.3) from Bruker Daltonics with error limits below or equal to  $15 \mu\text{g C L}^{-1}$ .

### Community of sulfate-reducing and SOB

Sediment and biofilm samples were taken in sterile Falcon tubes. DNA extraction and data analysis were performed as described in detail by Ionescu *et al.* (2012). Tag pyrosequencing for bacterial diversity, using primer sets

28F and 519R (Lane, 1991), was done by MrDNA (Shallowater, TX), using a Roche 454 FLX Genome Sequencer (Branford, CT). The obtained sequences were screened for bacteria affiliated to sulfur-oxidizing and SRB.

### *In situ* microsensor measurements

For *in situ* microsensor measurements, Clark-type oxygen (Revsbech & Ward, 1983),  $\text{H}_2\text{S}$  (Jeroschewski *et al.*, 1996) and pH microelectrodes (Revsbech & Jørgensen, 1986) were used. The microsensors had a tip diameter between 20 and 50  $\mu\text{m}$ . To obtain an estimation of salinity inside the microbial mat, the profiler was additionally equipped with a salinity mini-sensor with a tip diameter of 1.5 mm using the measuring principle as described in detail in Häusler *et al.* (2014). This sensor is able to measure salinities of 0–350  $\text{g L}^{-1}$  NaCl (high range sensor). However, in DSW a decrease in sensor signal is observed in liquids containing > 75% DSW due to its above described unique salt composition. Thus, accurate calibrations cannot be obtained and only the raw signal was qualitatively compared to the reference site. For accurate salinity determination a second salinity sensor was used (low range sensor) with the same measuring principle as the first but adjusted to measure linearly in salinities from freshwater to 70  $\text{g L}^{-1}$  TDS. Above this value it was out of range (O.R.) and showed a constant signal. All sensors were mounted on an autonomous profiling lander (Gundersen & Jørgensen, 1990; Wenzhöfer & Glud, 2002) to conduct measurements at the sediment–water interface in a white microbial mat located on a seepage area (hereafter WhMat1) and a Dead Sea reference site not influenced by emerging groundwater. Depth profiles were recorded with a spatial resolution of 100  $\mu\text{m}$ . The sensors were allowed to equilibrate in each depth for 5 s before the signal was recorded. Triplicate readings were averaged from each depth. For another white microbial mat located vertically on a cliff (hereafter WhMat2), the Diver-Operated Microsensor System (DOMS) was used (Weber *et al.*, 2007). There the oxygen profile and sulfide profile were measured subsequently, since this instrument allows the mounting of only one sensor at a time. The sensors were also allowed to equilibrate in each depth for 5 s and triplicate readings recorded.

### Microsensor calibration

Oxygen microsensors were calibrated prior to the measurement using a linear two-point calibration. The signal obtained in aerated DSW at *in situ* temperature represented the concentration corresponding to 100% air saturation. The concentration of oxygen was then determined

at corresponding temperatures in triplicate using a modified Winkler protocol for DSW (Nishri & Ben-Yaakov, 1990). The reading in anoxic DSW and anoxic freshwater (both prepared by dissolution of 0.1 g sodium dithionate in 10 mL) was the same as in the deeper sediment layers and thus taken as zero oxygen. The H<sub>2</sub>S sensor was calibrated at *in situ* temperature (28 °C) in acidified spring water (pH 2) by adding increasing amounts of NaS solution. Aliquots were taken and fixed in 2% ZnAC solution (w/v) and determined afterwards with the colorimetric assay of Cline (1969). pH sensors were 2-point calibrated using commercial buffer solutions (Mettler Toledo). The salinity sensors were calibrated using a dilution series of DSW with de-ionized water.

### Sulfate reduction measurements

Intact cores were sampled by SCUBA divers at the different sites and transferred to the lab of the Hebrew University of Jerusalem within 12 h. To obtain a uniform salinity throughout each core, SRR were measured in WhMat1 sediment using the percolation technique described by De Beer *et al.* (2005). Two replicate cores were then percolated with twice the core volume using anoxic water (bubbled 1 h with N<sub>2</sub> gas) with either a high salinity of 276 g L<sup>-1</sup> TDS obtained by mixing 20% spring water and 80% Dead Sea (v/v) or a low salinity of 90 g L<sup>-1</sup> (80% spring water and 20% DSW). Afterwards the percolation of each core was repeated with the same water containing 25 kBq mL<sup>-1</sup> of <sup>35</sup>SO<sub>4</sub><sup>2-</sup>. The cores were then incubated for 6–8 h at 27 °C. The incubations were terminated by slicing the cores at 1-cm intervals and suspending the sediment into equal amounts of 20% (w/v) Zn-acetate. <sup>35</sup>S reduction was determined and calculated using the cold chromium distillation procedure after Kallmeyer *et al.* (2004). In sediment cores from the Dead Sea reference site as well as from a spring outlet covered with diatoms (hereafter DMat), core percolation was not possible and thus SRR were determined using the whole core injection method (Fossing & Jørgensen, 1989). Radioactively labeled sulfate solution (25 µL of 50 kBq µL<sup>-1</sup> of <sup>35</sup>SO<sub>4</sub><sup>2-</sup>) was injected at 1-cm intervals into the cores. Afterwards the cores were incubated, sliced and incubation was terminated as described above.

A third experiment was conducted in sediment slurries from the top 3- to 4-cm surface sediment of WhMat1. The sediment was sampled with cores and stored for 1 week at 4 °C before the measurements were performed. Sediment was homogenized under N<sub>2</sub> atmosphere. Spring water (30 g L<sup>-1</sup> TDS) was mixed with DSW (338 g L<sup>-1</sup> TDS) to obtain a salinity gradient ranging from pure spring water to 100% DSW. Then the water mixtures

were amended with lactate, acetate, propionate and butyrate each, to a final concentration of 0.1 mM. Then 4 mL of sediment and 16 mL of Spring-DSW mixture at the defined salinity were added to serum bottles, perched with N<sub>2</sub> gas and vigorously shaken. Before adding 20 µL of 50 kBq µL<sup>-1</sup> of <sup>35</sup>SO<sub>4</sub><sup>2-</sup>, the vials were incubated for 3 h at 27 °C to enable salinity adaptation. Incubation time ranged from 12 to 36 h. The incubations were terminated by injection of 5 mL 20% Zn-Acetate and SRR were determined as described above.

### Sediment porosity and porewater

Efficient porosity of the sediment for calculation of SRR was determined by the weight loss of sediment after drying at 70 °C for 48 h. Porewater was collected from each site using core sections of 1-cm intervals and centrifuging each section 15 min at 11 100 g. Sulfate concentration in the porewater was determined in diluted samples using an ion chromatograph (761 Compact IC; Metrohm, Filderstadt, Germany). Salinity determination was done by gravimetric density measurement and calculation assuming linear mixing of pure groundwater from the springs and DSW.

### Flux calculations

Diffusive fluxes were calculated according to Fick's first law of diffusion,

$$J = -\Phi D_{\text{eff}} \frac{\partial C_i}{\partial x} \quad (1)$$

where  $\Phi$  is the porosity of the microbial mat,  $D_{\text{eff}}$  is the effective diffusion coefficient in the microbial mat and  $dC/dx$  is the one-dimensional concentration gradient. Porosity in the microbial mat was assumed to be 0.9 (Jørgensen & Cohen, 1977; Jørgensen *et al.*, 1979; Wieland & Köhl, 2000).  $D_{\text{eff}}$  was determined as  $D_{\text{eff}} = D_0/\theta^2$ , where  $D_0$  is the diffusion coefficient in water at the given salinity and temperature, and  $\theta^2$  is tortuosity with  $\theta^2 = 1 - \ln(\Phi^2)$  (Berner, 1980; Boudreau, 1996). Since the low range salinity sensor signal was constant at 60‰ inside the microbial mat, it is unlikely that temperature and salinity changed within the approximately 2-mm-thick microbial mat. Thus,  $D_0$  was also assumed to be constant, and  $D_0$  for oxygen and sulfide at 60‰ salinity and 28 °C was taken from the tables of seawater and gases (<https://www.unisense.com/support>). Total sulfide concentrations at each depth were calculated from the local H<sub>2</sub>S concentrations and pH values as described by Jeroschewski *et al.* (1996). For pKs estimation, the ionic strength at each point of the profile was calculated

**Table 1.** Physico-chemical properties of the Dead Sea and pure spring water

System	Sample	Temperature (°C)	pH	Eh (mV)	TDS (g L <sup>-1</sup> )	SO <sub>4</sub> <sup>2-</sup> (mM)	H <sub>2</sub> S <sub>tot</sub> (μM)	DIC (mM)	DOC (mM)	TDN (mM)	DOC/TDN	NH <sub>4</sub> (mM)
	Dead Sea*	27.5	6.16	90	338.0	1.39	0	1.05	1.36	0.88	1.5	0.43
North springs	Spring 01	24	7.16	-180	12.8	3.50	NA	3.36	NA	NA	NA	NA
	Spring 07	29.3	7.08	-80	24.8	10.71	57.0	4.2	0.56	0.1	5.3	NA
South springs	WhMat1	28.2	6.91	NA	30.9	2.68	54.0	3.13	0.34	0.12	2.7	0.16
	DMat	29.1	6.93	NA	58.8	2.13	NA	5.56	0.33	0.12	2.6	0.68
	WhMat2	27.7	6.70	-130	50.2	3.04	63.0	2.77	0.43	0.2	2.1	0.16
	RockMat	28.7	6.70	-147	54.9	3.39	80.0	3.05	0.48	0.23	2.1	0.11

\*Data taken from Ionescu *et al.* (2012).

assuming linear mixing between the spring water source and DSW according to the salinity profile. The pKs were then estimated according to the obtained ionic strength of all ions at each point of the profile using the formula for high ionic strength NaCl solutions at 28 °C provided by Hershey *et al.* (1988). For oxygen flux calculation at the reference site, according to Gat & Michal (1991),  $D_0$  of DSW was estimated to be 0.36 of the diffusion coefficient of freshwater at *in situ* temperature. The latter  $D_0$  was taken from the tables of Seawater and Gases (<https://www.unisense.com/support>).

### Consideration of porewater advection

In the presence of advective porewater flow the diffusive flux cannot be calculated from Eqn. (1). Instead, a 1D numerical transport-reaction model was set up using the finite element program COMSOL MULTIPHYSICS® 4.3. Steady-state conditions across the thin mats can be assumed, as the relatively thin mats (1–2 mm) are expected to respond within tens of seconds to minutes. Therefore the governing equation is

$$-\Phi D_{\text{eff}} \frac{\partial^2 C_i}{\partial x^2} + \Phi u \frac{\partial C_i}{\partial x} = R_i \quad (2)$$

where  $u$  is the porewater velocity and  $R$  the reaction rate (per volume mat or sediment) of the compound  $i$  described by Michaelis–Menten kinetics (half saturation constant: 10 μmol L<sup>-1</sup>). Since WhMat1 was covered with a microbial mat of potential sulfide oxidizers, Eqn. (2) was solved for concentrations of H<sub>2</sub>S and O<sub>2</sub> and the two equations were coupled assuming either complete oxidation of sulfide (H<sub>2</sub>S + 2O<sub>2</sub> → SO<sub>4</sub><sup>2-</sup> + 2H<sup>+</sup>) or oxidation of sulfide to elemental sulfur (2H<sub>2</sub>S + O<sub>2</sub> → 2S + 2H<sub>2</sub>O), so that either  $R_{O_2} = 2 \times R_{H_2S}$  or  $2 \times R_{O_2} = R_{H_2S}$ . Constant concentrations of O<sub>2</sub> and H<sub>2</sub>S were set as upper and lower boundaries, respectively. Subsequently, the porewater velocity in the model was adjusted until the best match of modeled and measured concentrations was found. Then, the total fluxes were extracted.

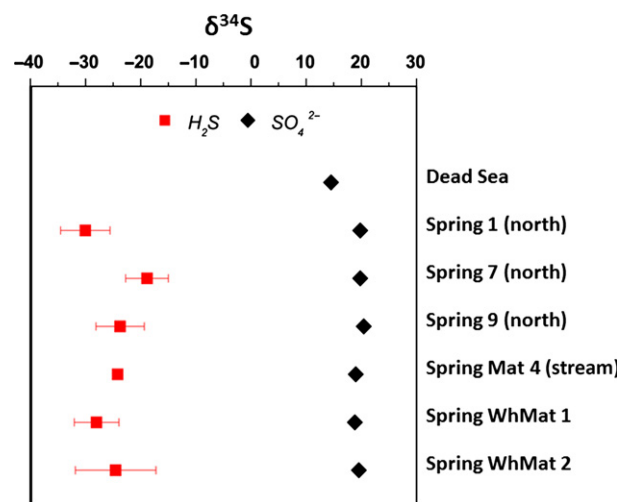


**Fig. 1.** Isotopic composition of sulfide and sulfate obtained from the Dead Sea and pure spring water samples. The error bars represent variation between triplicate samples from the same point. The variations for sulfate are small and enclosed within the symbol.

## Results

### Sulfur isotopes and physico-chemical parameters

The physico-chemical parameters of the spring waters sampled in the northern and southern system, respectively, are summarized in Table 1. Compared with the Dead Sea, the springs contain up to five times more sulfate and are all significantly less saline, significantly sulfidic, and have a higher pH. Total dissolved organic carbon (DOC) and total dissolved nitrogen (TDN) are higher in the Dead Sea, whereas inorganic carbon (DIC) is higher in the groundwaters. The DOC/TDN ratio is < 3, indicating that most of the TDN exists in inorganic form, fitting well with the high ammonia values obtained.

$\delta^{34}\text{S}$  signatures of sulfate in the spring water range from 19‰ to 20‰, whereas  $\delta^{34}\text{S}$  signatures of sulfide range from -19‰ to -30‰ (Fig. 1). The overall

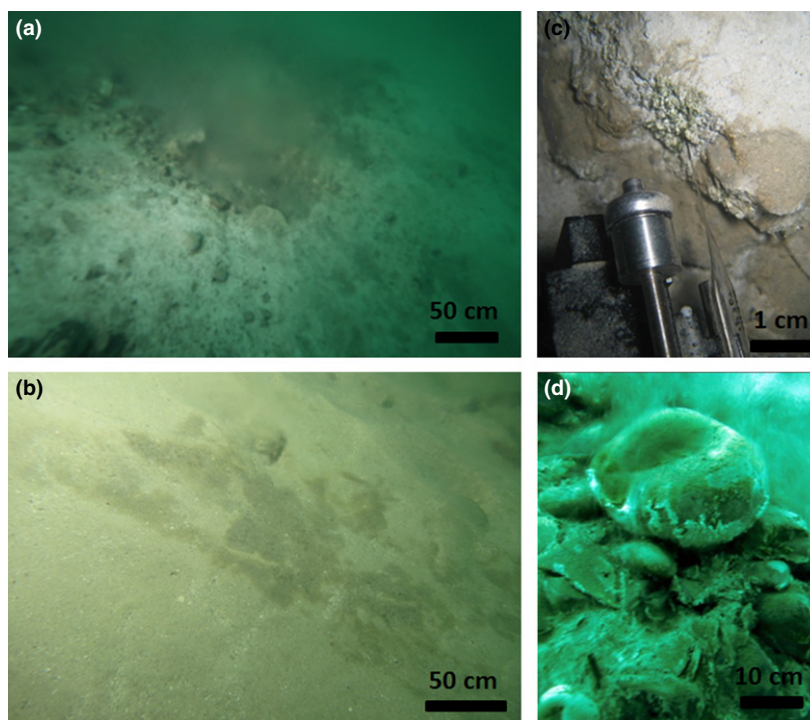


**Fig. 2.** Images showing the different microbial mats found in the underwater springs. WhMat1 (a) and DMat (b) cover several square meters of sediment, (c) WhMat2 and (d) Mat4.

fractionation  $\Delta^{34}\text{S}$  ( $\delta_{\text{sulfate}}^{34} - \delta_{\text{sulfide}}^{34}$ ) between sulfide and sulfate ranges from 39‰ to 50‰ in the various springs.

### Microbial mats and their respective sulfur-metabolizing bacterial community

Our sampling and measurements were focused on four microbial mats, all of which were exposed to spring water seepage. Two of the microbial mats spread over several square meters at spots where groundwater slowly seeps out of the sediment. At the first site, the sediment was covered by a 1- to 2-mm-thick white microbial mat (WhMat1, Fig. 2a), whereas the sediment at the second site was covered by a brownish mat, mainly formed by diatoms (DMat, Fig. 2b). A microbial mat similar to WhMat1 was found on a vertical cliff (WhMat2, Fig. 1c). A fourth type of microbial mat was found on cobble located inside a fast flowing jet of 1–2 m in diameter (hereafter RockMat, Fig. 2d).

Sequences matching the 16S rRNA gene of known SRB and SOB were detected in all microbial mats as well as in the Dead Sea (Fig. 3). Generally, sequence abundance of SRB and SOB was higher in the microbial mats than in the Dead Sea, indicating that the conditions for both groups are more favorable in the spring environments. Comparing the springs with each other revealed that the highest SOB and SRB richness can be found in RockMat and WhMat1, which were clearly dominated by sequences related to SOB. Specifically, in WhMat1 the dominating

SOB taxa are closely related to the *Sulfurimonas* and *Sulfurovum* genera, which are also found in RockMat, although sequences related to the green sulfur bacterium *Prosthecochloris* are most abundant in the latter. *Thiobacillus*-like sequences represent the main SOB in both DMat and WhMat2, with *Acidithiobacillus* being additionally detected in the former. Among the SRB, WhMat1 and RockMat are dominated by a single genera MSBL7, which belongs to the *Desulfobulbaceae* family and has no cultured representatives. In contrast, sequence abundance and taxa numbers of SOB and SRB are remarkably reduced in DMat and WhMat2, where the sole sequences related to SRB cluster to the *Desufosporosinus*. The only SRB detected in the Dead Sea reference site clusters to the *Desulfobulbus* genus.

### In situ microsensor measurements

*In situ* microsensor measurements performed in WhMat1 (Fig. 4a and b) and at a reference site not exposed to spring water seepage (Fig. 4c and d) revealed clear differences. The impact of the spring water seepage at WhMat1 can be clearly seen by the sharp decrease in the signal of the high range salinity sensor (Fig. 4b). The short increase of sensor signal before its decrease is a result of the sensor response when exposed to pure DSW: with increasing salinity, it shows an increasing signal starting from freshwater to 75‰ DSW and decreases at higher TDS again. According to this, salinity already starts to

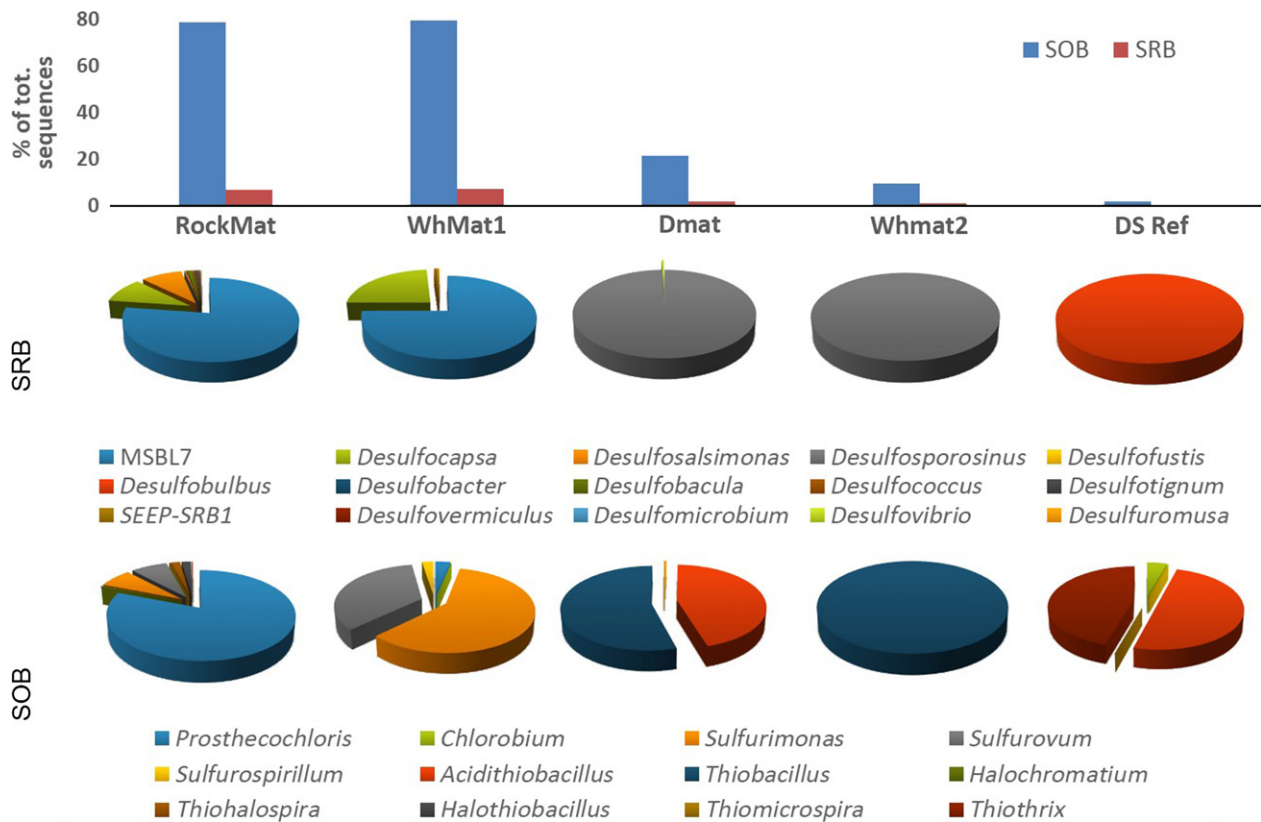


**Fig. 3.** Graphical representation of the sequence frequency of SRB and SOB in the studied microbial mats and the Dead Sea (DS Ref) sediment (upper). The lower panels show the relative sequence frequency of detected genera in each sample.

decrease 4 mm above the microbial mat, which is also seen in the low range salinity profile when the sensor reached its maximum of detectable salinity (Fig. 4b). Salinity inside the microbial mat is constant at around  $60 \text{ g L}^{-1}$  and decreases inside the sediment to  $40 \text{ g L}^{-1}$ , which is in agreement with the value measured in the pure spring water from this site ( $30 \text{ g L}^{-1}$ , Table 1). The data from the reference site shows that the sediment does not interfere with the readings of the salinity sensor (Fig. 4c).

In WhMat1, pH increased from 6.1 to 6.6 and redox potential decreased steeply at the surface of the microbial mat. Oxygen concentrations followed the same shape as redox potential and decreased from  $49 \mu\text{M}$  (DSW air saturation) to complete depletion at a depth of 2 mm inside the sediment (Fig. 4a). Sulfide was consumed in the 2mm oxic zone, indicating direct sulfide oxidation with oxygen as electron acceptor. Measured concentrations were compared with profiles calculated using a numerical model and a porewater flow out of the sediment of  $0.1 \mu\text{m s}^{-1}$ . The complete oxidation of sulfide to sulfate ( $\text{H}_2\text{S} + 2\text{O}_2 \rightarrow \text{SO}_4^{2-} + 2\text{H}^+$ ) was found to have the best fit to the measured data (Fig. S2a). Total fluxes of oxygen and sulfide calculated considering both diffusion and

advection, were  $12.12$  and  $6.06 \text{ mmol m}^{-2} \text{ day}^{-1}$ , respectively. When using alternative stoichiometry, that is the oxidation of sulfide to elemental sulfur ( $2\text{H}_2\text{S} + \text{O}_2 \rightarrow 2\text{S} + 2\text{H}_2\text{O}$ ), the modeled and measured  $\text{O}_2$  profiles closely matched if a porewater flow of  $20 \mu\text{m s}^{-1}$  was used; however, the modeled  $\text{H}_2\text{S}$  concentrations deviated significantly from the measured values (Fig. S2b).

In WhMat2, oxygen was depleted within the first 0.2 mm of the mat (Fig. 5). Here, the overlapping  $\text{H}_2\text{S}$  and oxygen profile also indicates that sulfide was oxidized with oxygen; however, since salinity and pH were not measured in this mat (due to technical limitations), we do not provide any flux calculations.

In contrast to WhMat1 and WhMat2, oxygen at the reference site penetrated around 1 cm into the sediment. Diffusive oxygen uptake was estimated to be  $0.46 \text{ mmol m}^{-2} \text{ day}^{-1}$  and was thus 36 times lower than the oxygen consumption measured in the WhMat1. Sulfide was not detectable and pH was constant at 6.1.

### Sulfate reduction activity

SRR in the cores collected from WhMat1 were extremely low at both  $90$  and  $276 \text{ g L}^{-1}$  TDS, range  $0.02$ – $1.21$  and

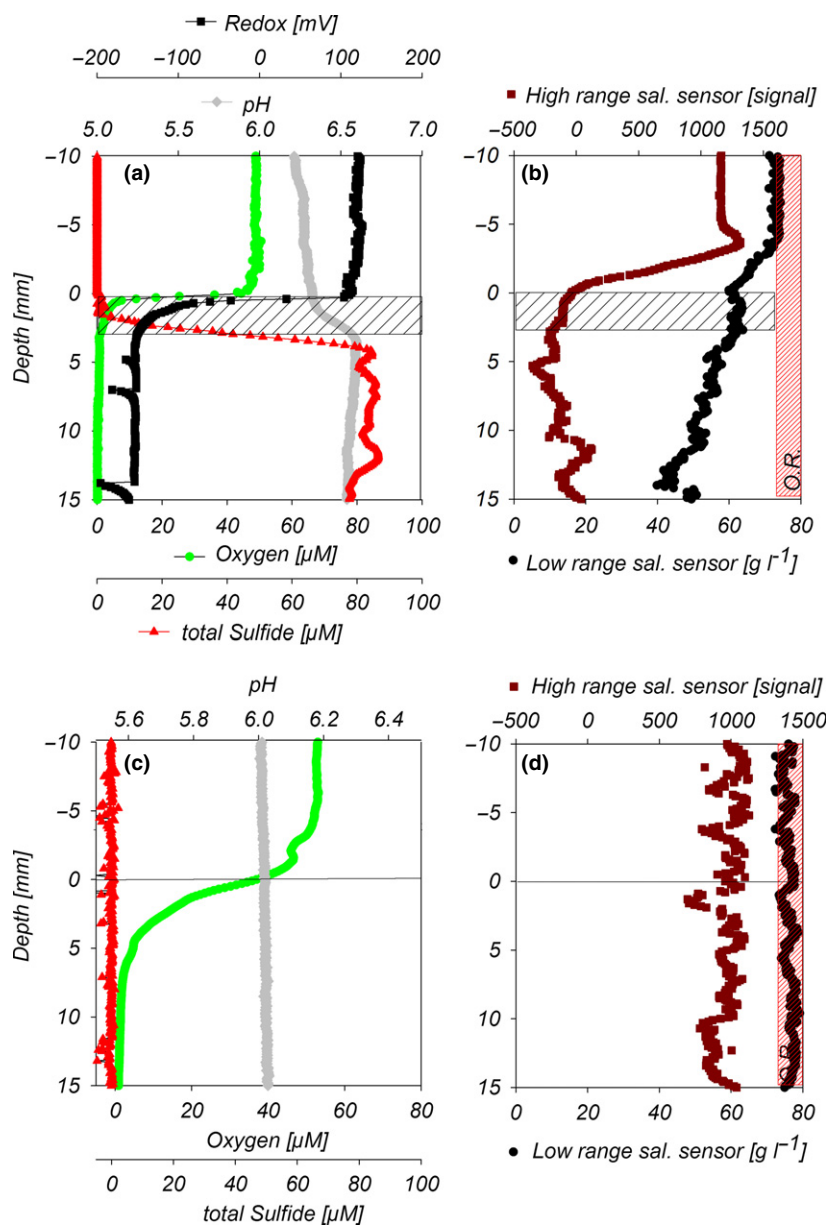


**Fig. 4.** Microsensor profiles measured *in situ* in the WhMat1 microbial mat (a and b) and the Dead Sea reference site (c and d). Shaded area in (a) and (b) corresponds to the location of the microbial mat, whereas the line in (c) and (d) indicates the sediment surface. The low range salinity sensor is only able to measure up to  $70 \text{ g L}^{-1}$ , beyond this salinity, it is O.R.

$0.001\text{--}1.06 \text{ nmol cm}^{-3} \text{ day}^{-1}$ , respectively (Fig. 6). In the core collected from DMat, the salinity was constant throughout the core at  $186 \text{ g L}^{-1}$  as determined after the incubation. SRR in DMat was slightly higher than in WhMat1 cores and ranged from  $0.006$  to  $2.8 \text{ nmol cm}^{-3} \text{ day}^{-1}$ . Highest SRR rates of up to  $10.1 \text{ nmol cm}^{-3} \text{ day}^{-1}$  were detected in the Dead Sea reference site. Although care was taken to obtain replicate cores close to each other, no clear pattern of SRR with depth could be observed, indicating an extremely heterogeneous spatial distribution of sulfate-reducing microorganisms in both the Dead Sea and spring water sediments. Cumulative, depth-integrated rates ( $0\text{--}10 \text{ cm}$ ) revealed no clear

differences in the total SRR between high and low salinity in WhMat1 sediment (Fig. 6). Nevertheless, the highest depth integrated rates of  $35.1 \mu\text{mol m}^{-2} \text{ day}^{-1}$  were three orders of magnitude lower than the total sulfide flux of  $6.06 \text{ mmol m}^{-2} \text{ day}^{-1}$  determined by microsensors from the same site.

The effect of salinity on SRR was further tested at a higher resolution in a slurry experiment performed with sediment collected from the upper 2–3 cm of WhMat1 (Fig. 7). To enhance SRR, lactate, acetate, propionate and butyrate ( $0.1 \text{ mM}$  final concentration of each) were added to the slurries. Generally, the rates were in the lower range of those determined in the core incubations

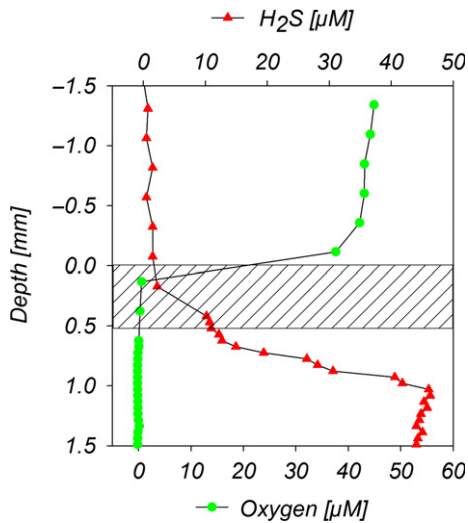


**Fig. 5.**  $\text{H}_2\text{S}$  and oxygen microsensor profiles measured *in situ* in the WhMat2 microbial mat located vertically on a cliff where spring water flow passed parallel. Shaded area indicates position of the biofilm.

from this site, with a maximum of  $0.05 \text{ nmol cm}^{-3} \text{ day}^{-1}$ . Replicate incubations showed a similar pattern at low and intermediate salinities. Among the different salinities tested, the highest SRR were observed in samples incubated at  $90\text{--}120 \text{ g L}^{-1}$  TDS; however, in two incubations of  $276$  and  $300 \text{ g L}^{-1}$  TDS, respectively, elevated activity was detected as well.

The compounds identified by FT-ICR-MS were divided in categories according to where they were found. Unique compounds are those which were found only in the springs (1806), only in the aquifers (238) or only in the Dead Sea (89). Compounds identified in the three datasets (5711) are considered to be refractory, as they seem to be resistant to microbial degradation. A total of 2575 compounds from the aquifers are also found in the springs (but not in the Dead Sea) and 1563 compounds originating in the springs are also present in the Dead Sea (Fig. S3).

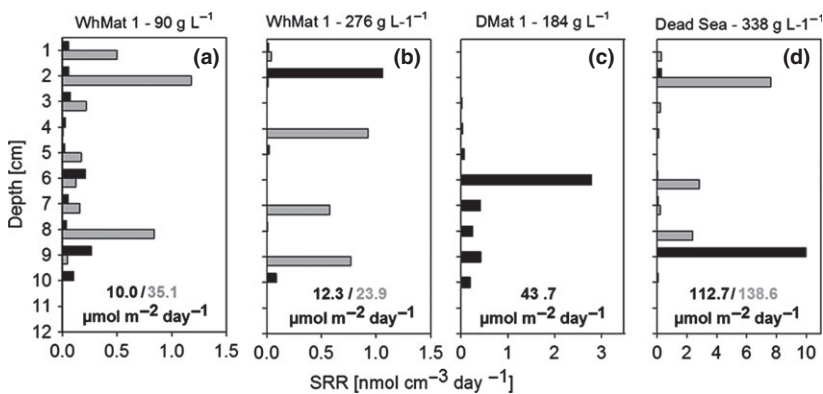


**Fig. 6.** SRR determined in cores from the WhMat1 site by percolation with low saline water (a) and high saline water (b). SRR in the DMat site (c) and Dead Sea reference site (d) were determined by the injection technique. Gray and black bars correspond to the values obtained in the replicate cores from each site with the depth-integrated rates shown in the respective color at the bottom of each graph.

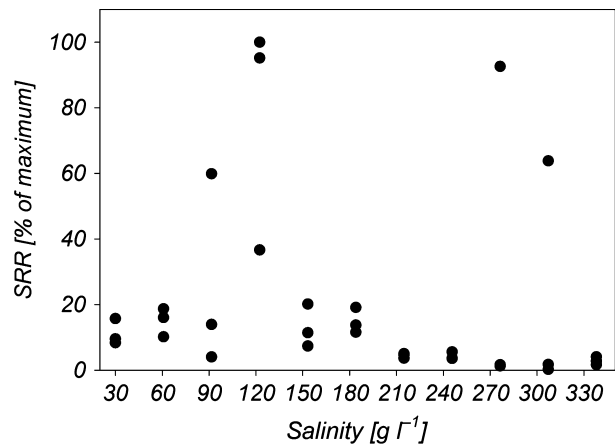


**Fig. 7.** Relative sulfate reduction activity (SRR) determined in a slurry experiment in triplicate over a salinity range from pure spring water ( $30 \text{ g L}^{-1}$  TDS) to pure Dead Sea water ( $340 \text{ g L}^{-1}$  TDS). Slurries were amended with lactate, acetate, propionate and butyrate,  $1 \text{ mM}$  each.

## Discussion

Our results showed that the sulfide provided by the springs is of biological origin. This can be concluded from the high fractionations between coexisting sulfide and sulfate in the spring waters, where  $\Delta^{34}\text{S}$  ( $\delta_{\text{sulfate}}^{34} - \delta_{\text{sulfide}}^{34}$ ) ranged from  $39\text{‰}$  to  $50\text{‰}$ . Such high fractionations (and up to about  $70\text{‰}$  in other cases) usually only occur during bacterial sulfate reduction (Brunner & Bernasconi, 2005; Canfield *et al.*, 2010; Sim *et al.*, 2011). Thermochemical sulfate reduction usually does not lead to high fractionations (Machel *et al.* 1995). Biological sulfate reduction is further supported by the presence of OM alongside sulfate, in the spring waters (Table 1). The increased DIC concentrations as well as the high concentrations of ammonia in the spring waters (Table 1) also point to bacterial degradation of OM, as previously concluded (Ionescu *et al.*, 2012). Biological sulfate reduction also occurs in the subsurface flow path of (thermal)

springs elsewhere at the Dead Sea (Gavrieli *et al.*, 2001; Avrahamov *et al.*, 2014). However, in these springs, isotope fractionation between sulfide and sulfate was only *c.* 30‰ (Gavrieli *et al.*, 2001, and references therein), whereas we measured up to 50‰ in the springs investigated here. The magnitude of sulfur isotope fractionations was suggested to depend on microbial metabolism and carbon sources (Detmers *et al.*, 2001; Sim *et al.*, 2011), rate of sulfate reduction (Habicht & Canfield, 2001), temperature (Brüchert *et al.*, 2001), amount of available sulfate (Habicht *et al.*, 2002), sulfur disproportionation (Canfield & Thamdrup, 1994; Canfield *et al.*, 1998) as well as reoxidation of sulfide by SRB during sulfate reduction (Eckert *et al.*, 2011). While future measurements are needed to show the activity of SRB and SOB in the spring water, our results strongly support the activity of sulfate-reducing microorganisms along the subsurface flow path of the springs through the Quaternary sediment body.

The SRR measurements conducted in this study (Fig. 6) indicated that the SRB community detected by 16S rRNA gene analysis (Fig. 3) is indeed active both in the spring sediments and the Dead Sea. The SRR in the Dead Sea was up to 10.1 nmol cm<sup>-3</sup> day<sup>-1</sup>, in the lower range of those mentioned by Oren (1988) in the Dead Sea shore sediment. Thus although no SRB have been isolated so far from the Dead Sea (Oren, 2010), our results confirm the existence of an active sulfate-reducing community adapted to the harsh conditions in the lake. Members of the *Desulfobulbus* genus were the only sequences detected in the Dead Sea sediment, which could be associated with known SRB (Fig. 3). Although members of the *Desulfobulbaceae* family are generally not halophilic (Kuever *et al.*, 2005), sequences of this family were found on the floor of the extreme Mg<sup>2+</sup>-rich hypersaline Bannock Basin, Mediterranean Sea (Daffonchio *et al.* 2006). They were also detected in extremely hypersaline evaporation pans in South Africa (Roychoudhury *et al.* 2013). Furthermore, the *Desulfobulbaceae* family consists mostly of incomplete oxidizers (Kuever *et al.*, 2005), which are generally observed to be more halotolerant than complete oxidizers (Oren, 1999, 2011). Therefore, extreme halophilic members of the *Desulfobulbus* genus could indeed be responsible for the activity observed in the Dead Sea. However, the SRR in the Dead Sea were very low compared with other extremely hypersaline environments such as lake Tanatar in the Kulunda Steppe (< 475 g L<sup>-1</sup> TDS), where SRR of 12–423 nmol cm<sup>-3</sup> day<sup>-1</sup> were measured (Foti *et al.* 2007). High SRR were also measured in a saltern pan systems in South Africa (422 g kg<sup>-1</sup> TDS, 27–3685 nmol cm<sup>-3</sup> day<sup>-1</sup>; Porter *et al.* 2007). Thus assuming that the Dead Sea SRB are adapted to the unusual salt composition of the lake,

the high salinity in the Dead Sea of 340 g L<sup>-1</sup> TDS (274 g kg<sup>-1</sup> TDS) is unlikely to limit SRR. The low sulfate concentrations in the Dead Sea (above 1 mM, Table 1) should also not limit SRR (Roychoudhury *et al.*, 1998). However, it is well known that OM availability and quality strongly affect SRR in marine and hypersaline environments (Schubert *et al.*, 2000; Niggemann *et al.*, 2007; Glombitza *et al.*, 2013). Therefore, the low SRR measured in the Dead Sea sediment could be a consequence of the general lack of primary production and thus low input of fresh organic carbon to the sediment. Extensive primary production by the algae *Dunaliella* was only observed twice in recent history, in 1980 and 1992 (Oren, 2010). The low carbon input from the water column to the sediment is further supported by the low benthic oxygen uptake of 0.46 mmol m<sup>-2</sup> day<sup>-1</sup> measured in the reference site. Such rates are comparable to deep sea environments where carbon flux to the sediment is low (Glud *et al.*, 1994).

Interestingly, SRR were even lower in the spring sediment than in the Dead Sea sediment (Fig. 6). This was unexpected since the spring water locally reduces the extreme salinity of the Dead Sea (Fig. 4b; Häusler *et al.* 2013), which appears to allow for the proliferation of more taxa of SRB, especially seen in WhMat1 and RockMat (Fig. 3). Also, in contrast to the Dead Sea, SRR in the spring sediment are most likely not limited by OM supply. Part of the OM delivered by the springs originates from the aquifer, or from the underwater flow path. Most of it cannot be traced back in the DSW column, suggesting that this OM is bioavailable and is rapidly consumed either in the spring sediments or in the Dead Sea, very close to the sediment (Fig. S3). Furthermore, we were not able to enhance SRR by the addition of known substrates for SRBs (lactate, acetate, propionate and butyrate). We therefore suggest that extreme spatio-temporal salinity fluctuations in the spring sediments can explain these low SRR. Such salinity fluctuations are indicated by measurements of variable flow in the spring system (Häusler *et al.*, 2014) and are further supported by salinity profiles measured subsequently over several hours in the same spot of WhMat1 (Fig. S4). Due to the fluctuating spring flow, pressure-induced convective circulation similar to other seeping systems (Wenzhöfer *et al.*, 2000), or haline convection as modeled from estuarine environments (Webster *et al.*, 1996) are also likely to occur, leading to DSW invading the sediment. This will lead to extreme spatio-temporal salinity fluctuations in the system, allowing development of microniches of different salinity in the spring sediment, which can be occupied by SRB possessing different salinity optima. Indeed, the SRB community in WhMat1 sediment appears to harbor two subpopulations with a low and high salinity optimum of

90–120 and 280–300 g L<sup>-1</sup> TDS, respectively (Fig. 7). A heterogeneous distribution of these SRB groups may be the reason for the heterogeneous SRR detected in the cores (Fig. 6). However, despite the availability of multiple environmental niches, continuous salinity fluctuations will require constant metabolic adjustment of the cells to the prevailing conditions. For example, upon salinity increase, the sulfate reducer *Desulfovibrio vulgaris* shows an up-regulation of the ATPase gene at the transcript and protein level (Mukhopadhyay *et al.*, 2006), indicating a general higher energy demand in salt-stressed SRB. The increase in energy demand is likely a consequence of cellular adjustments, including the synthesis or uptake of organic solutes to achieve osmotic equilibrium with the ambient medium, cell membrane changes as well as up-regulation of ion efflux systems (Mukhopadhyay *et al.*, 2006). Constant salinity fluctuations thus dramatically increase the overall maintenance energy of the SRB population in the spring system, resulting in energy shortage for cell division, and may limit the population size of SRB since this physiological group only obtains a little energy from their metabolism (Oren, 1999; 2011). An overall low population size may thus be responsible for the low SRR observed in the surface sediment of the springs (Fig. 6), and may also explain the extreme heterogeneity in the slurry experiment (Fig. 7).

The SOB community is independent of the local SRR in the spring surface sediment and relies of sulfide supplied by the spring water. This can be concluded from the low maximal depth integrated SRR of 35.1  $\mu\text{mol m}^{-2} \text{day}^{-1}$ , which was three orders of magnitude lower than the sulfide flux of 6.06  $\text{mmol m}^{-2} \text{day}^{-1}$  measured in the same area. The sulfide supplied by the spring water is aerobically oxidized by the SOB community at the interface between spring- and DSW (Figs 4 and 5), where oxygen is present and an overall reduced salinity allows their development. Since aerobic sulfide oxidation delivers far more energy than sulfate reduction (Oren, 1999; 2011), the SOB community probably has sufficient energy to survive the salinity fluctuations in the spring system, and thus allows the buildup of the high biomass. We suggest that the main driving factor for the development of the high biomass of SOB in the spring system of the Dead Sea is a local reduction in salinity and the external supply of sulfide, which is aerobically consumed with oxygen supplied from the Dead Sea.

Although all springs may experience large spatio-temporal salinity fluctuations, we suggest that the observed differences between the community structures of SOB and SRB in the distinct microbial mats (Fig. 3) are likely to be a result of different mean salinities. On average the salinity is probably lowest around RockMat and in WhMat1, where most taxa are found, whereas salinity is

on average higher in DMat and WhMat2, allowing only the existence of specific, presumably more halotolerant SRB and SOB taxa of *Desulfosporosinus* and *Thiobacillus/Acidithiobacillus*, respectively. Percolation of the core obtained in the DMat was not possible due to its low permeability. The lower permeability leads to reduction in spring water flow velocity through the sediment, which in turn will result in higher salinities inside and above the sediment. Indeed, the porewater salinity of DMat was about 184 g L<sup>-1</sup> TDS throughout the core, much higher than the porewater salinity in WhMat1 (about 60 g L<sup>-1</sup> TDS, Fig. 4), which was dominated by SOB of the *Sulfurimonas* and *Sulfurovum* genera (Fig. 3). RockMat was located in a fast flowing stream where high spring water up-flow velocities of 5–25 cm s<sup>-1</sup> lead to an extensive salinity reduction around the rock surface (Häusler *et al.*, 2014). The high salinity in DMat could explain the general absence of the *Sulfurimonas*- and *Sulfurovum*-like bacteria at this site. Isolates of the *Sulfurimonas* and *Sulfurovum* genera were shown to tolerate a maximum salinity of 60 g L<sup>-1</sup> TDS (Inagaki *et al.*, 2003, 2004). It is therefore also likely that the SOB belonging to the *Acidithiobacillus*, *Thiobacillus* genera and the SRB belonging to the *Desulfosporosinus* genus detected solely in DMat and WhMat2 may be more halotolerant than the SOB and SRB detected in WhMat1. Bacteria related to the genus *Acidithiobacillus* were previously enriched at 4 M NaCl from hypersaline habitats (Sorokin *et al.*, 2006). Although species of the *Desulfosporosinus* (SRB) and *Thiobacillus* (SOB) genera are generally not halophilic (Kelly *et al.*, 2005; Spring & Rosenzweig, 2006), our results suggest that these genera may harbor halophilic members. Thus, overall the community structure of SRB and SOB in the different microbial mats seems to be controlled by salinity, in agreement with other studies showing a strong effect of salinity on community composition (Freitag *et al.*, 2006; Abed *et al.*, 2007). Differences in mean salinity are likely a result of different sediment permeabilities in the distinct areas affecting spring water input and thus salinity reduction.

In conclusion, we were able to demonstrate that most of the sulfide, which is aerobically consumed by sulfide-oxidizing bacteria in WhMat1 and WhMat2, is produced along the subsurface flow path of the spring water and only a little production occurs in the surface sediments of the springs, presumably due to extensive salinity fluctuations limiting local SRR. Thus, the main factors for the high abundance of SOB in the system are a local salinity reduction as already concluded (Häusler *et al.*, 2014) and the external supply of reduced substances from the spring water as shown here. We suggest that the reason for the different dominance of specific groups of SRB and SOB in the various microbial mats is a consequence of

different flow regimes of spring water in the system and thus differences in salinity. In addition, our results indicate that there is an active, extremely halophilic SRB community in the sediments of the Dead Sea which is not affected by spring water seepage. The ability of the SRB in the Dead Sea as well as the microorganisms in the springs to tolerate continuous or temporal exposures to high concentrations of divalent cations (*c.* 2 M Mg<sup>2+</sup> and 0.5 M Ca<sup>2+</sup>) warrants further investigation. More studies about the groundwater flow and the specific micro-environments are also needed to fully understand the dynamics of the system.

## Acknowledgements

This study was financially supported by the Max-Planck-Society and the SUMAR project (BMBF grant code: 02WM0848). We would like to acknowledge Benjamin Brunner for the isotope analysis. We also want to thank Christian Lott from the HYDRA Institute (Elba) for his support during diving and underwater videography. Furthermore, we would like to thank Shiri Meshner for providing us with lab space in the Ein Gedi lab of The Dead Sea and Arava Science Center. We are also deeply grateful for field assistance by Yaniv Munwes as well as the supply of lab equipment by Aharon Oren.

## References

- Abed RMM, Kohls K & De Beer D (2007) Effect of salinity changes on the bacterial diversity, photosynthesis and oxygen consumption of cyanobacterial mats from an intertidal flat of the Arabian Gulf. *Environ Microbiol* **9**: 1384–1392.
- Avrahamov N, Antler G, Yechieli Y, Gavrieli I, Joye SB, Saxton M, Turchyn AV & Sivan O (2014) Anaerobic oxidation of methane by sulfate in hypersaline groundwater of the Dead Sea aquifer. *Geobiology* **12**: 511–528.
- Berner RA (1980) *Early Diagenesis: A Theoretical Approach*. Princeton University Press, Princeton.
- Bodaker I, Sharon I, Suzuki MT *et al.* (2010) Comparative community genomics in the Dead Sea: an increasingly extreme environment. *ISME J* **4**: 399–407.
- Boudreau BP (1996) The diffusive tortuosity of fine-grained unlithified sediments. *Geochim Cosmochim Acta* **60**: 3139–3142.
- Brüchert V, Knoblauch C & Jørgensen BB (2001) Controls on stable sulfur isotope fractionation during bacterial sulfate reduction in Arctic sediments. *Geochim Cosmochim Acta* **65**: 763–776.
- Brunner B & Bernasconi SM (2005) A revised isotope fractionation model for dissimilatory sulfate reduction in sulfate reducing bacteria. *Geochim Cosmochim Acta* **69**: 4759–4771.
- Canfield DE & Thamdrup B (1994) The production of <sup>34</sup>S-depleted sulfide during bacterial disproportionation of elemental sulfur. *Science* **266**: 1973–1975.
- Canfield DE, Thamdrup B & Fleischer S (1998) Isotope fractionation and sulfur metabolism by pure and enrichment cultures of elemental sulfur-disproportionating bacteria. *Limnol Oceanogr* **43**: 253–264.
- Canfield DE, Farquhar J & Zerkle AL (2010) High isotope fractionations during sulfate reduction in a low-sulfate euxinic ocean analog. *Geology* **38**: 415–418.
- Cline JD (1969) Spectrophotometric determination of hydrogen sulfide in natural waters. *Limnol Oceanogr* **14**: 454–458.
- Daffonchio D, Borin S, Brusa T *et al.* (2006) Stratified prokaryote network in the oxic-anoxic transition of a deep-sea halocline. *Nature* **440**: 203–207.
- De Beer D, Wenzhöfer F, Ferdelman TG, Boehme SE, Huettel M, van Beusekom JEE, Böttcher ME, Musat N & Dubilier N (2005) Transport and mineralization rates in north sea sandy intertidal sediments, Sylt-Rømø basin, Wadden sea. *Limnol Oceanogr* **50**: 113–127.
- Detmers J, Brüchert V, Habicht KS & Kuever J (2001) Diversity of sulfur isotope fractionations by sulfate-reducing prokaryotes. *Appl Environ Microbiol* **67**: 888–894.
- Dittmar T, Koch B, Hertkorn N & Kattner G (2008) A simple and efficient method for the solid-phase extraction of dissolved organic matter (SPE-DOM) from seawater. *Limnol Oceanogr Methods* **6**: 230–235.
- Eckert T, Brunner B, Edwards EA & Wortmann UG (2011) Microbially mediated re-oxidation of sulfide during dissimilatory sulfate reduction by *Desulfobacter latus*. *Geochim Cosmochim Acta* **75**: 3469–3485.
- Elazari-Volcani B (1943a) A dimastigamoeba in the bed of the Dead Sea. *Nature* **152**: 301–302.
- Elazari-Volcani B (1943b) Bacteria in the bottom sediments of the Dead Sea. *Nature* **152**: 274–275.
- Elazari-Volcani B (1944) A ciliate from the Dead Sea. *Nature* **154**: 355.
- Fossing H & Jørgensen BB (1989) Measurement of bacterial sulfate reduction in sediments: evaluation of a single-step chromium reduction method. *Biogeochemistry* **8**: 205–222.
- Foti MJ, Sorokin DY, Zacharova EE, Pimenov NV, Kuenen JG & Muyzer G (2007) Bacterial diversity and activity along a salinity gradient in soda lakes of the Kulunda Steppe (Altai, Russia). *Extremophiles* **12**: 133–145.
- Freitag TE, Chang L & Prosser JI (2006) Changes in the community structure and activity of betaproteobacterial ammonia-oxidizing sediment bacteria along a freshwater–marine gradient. *Environ Microbiol* **8**: 684–696.
- Gat Joel R & Shatkay S (1991) Gas exchange with saline waters. *Limnol Oceanogr* **36**: 988–997.
- Gavrieli I, Yechieli Y, Halicz L, Spiro B, Bein A & Efron D (2001) The sulfur system in anoxic subsurface brines and its implication in brine evolutionary pathways: the Ca-chloride

- brines in the Dead Sea area. *Earth Planet Sci Lett* **186**: 199–213.
- Glombitza C, Stockhecke M, Schubert CJ, Vetter A & Kallmeyer J (2013) Sulfate reduction controlled by organic matter availability in deep sediment cores from the saline, alkaline Lake Van (Eastern Anatolia, Turkey). *Front Microbiol* **4**: 209.
- Glud RN, Gundersen JK, Barker Jørgensen BB, Revsbech NP & Schulz HD (1994) Diffusive and total oxygen uptake of deep-sea sediments in the eastern South Atlantic Ocean: *in situ* and laboratory measurements. *Deep Sea Res Part I Oceanogr Res Pap* **41**: 1767–1788.
- Gundersen JK & Jørgensen BB (1990) Microstructure of diffusive boundary layers and the oxygen uptake of the sea floor. *Nature* **345**: 604–607.
- Habicht KS & Canfield DE (2001) Isotope fractionation by sulfate-reducing natural populations and the isotopic composition of sulfide in marine sediments. *Geology* **29**: 555–558.
- Habicht KS, Gade M, Thamdrup B, Berg P & Canfield DE (2002) Calibration of sulfate levels in the Archean ocean. *Science* **298**: 2372–2374.
- Halas S & Szaran J (2001) Improved thermal decomposition of sulfates to SO<sub>2</sub> and mass spectrometric determinations of δ<sup>34</sup>S of IAEA-SO-5, IAEA-SO-6 and NBS-127 sulfate standards. *Rapid Commun Mass Spectrom* **15**: 1618–1620.
- Häusler S, Noriega-Ortega BE, Polerecky L, Meyer V, de Beer D & Ionescu D (2014) Microenvironments of reduced salinity harbour biofilms in Dead Sea underwater springs. *Environ Microbiol Rep* **6**: 152–158.
- Hershey JP, Plese T & Millero FJ (1988) The pK<sub>a</sub>\* for the dissociation of H<sub>2</sub>S in various ionic media. *Geochim Cosmochim Acta* **52**: 2047–2051.
- Inagaki F, Takai K, Kobayashi H, Nealson KH & Horikoshi K (2003) *Sulfurimonas autotrophica* gen. nov., sp. nov., a novel sulfur-oxidizing ε-proteobacterium isolated from hydrothermal sediments in the Mid-Okinawa Trough. *Int J Syst Evol Microbiol* **53**: 1801–1805.
- Inagaki F, Takai K, Nealson KH & Horikoshi K (2004) *Sulfurovum lithotrophicum* gen. nov., sp. nov., a novel sulfur-oxidizing chemolithoautotroph within the ε-Proteobacteria isolated from Okinawa Trough hydrothermal sediments. *Int J Syst Evol Microbiol* **54**: 1477–1482.
- Ionescu D, Siebert C, Polerecky L et al. (2012) Microbial and chemical characterization of underwater fresh water springs in the Dead Sea. *PLoS One* **7**: 21.
- Jeroschewski P, Steuckart C & Kühn M (1996) An amperometric microsensor for the determination of H<sub>2</sub>S in aquatic environments. *Anal Chem* **68**: 4351–4357.
- Jørgensen BB & Cohen Y (1977) Solar Lake (Sinai). 5. The sulfur cycle of the benthic cyanobacterial mats. *Limnol Oceanogr* **22**: 657–666.
- Jørgensen BB, Revsbech NP, Blackburn TH & Cohen Y (1979) Diurnal cycle of oxygen and sulfide microgradients and microbial photosynthesis in a cyanobacterial mat sediment. *Appl Environ Microbiol* **38**: 46–58.
- Kallmeyer J, Ferdelman TG, Weber A, Fossing H & Jørgensen BB (2004) A cold chromium distillation procedure for radiolabeled sulfide applied to sulfate reduction measurements. *Limnol Oceanogr Methods* **2**: 171–180.
- Kelly DP, Wood AP & Stackebrandt E (2005) Genus II *Thiobacillus* Beijerinck 1904. *Bergey's Manual of Systematic Bacteriology*, Vol. 2 Part C (Brenner DJ, Krieg NR, Staley JT & Garrity GM, eds), pp. 764–769. Springer, New York.
- Kuever J, Rainey FA & Widdel F (2005) Family II. *Desulfobulbaceae* fam. nov. *Bergey's Manual of Systematic Bacteriology*, Vol. 2 Part C (Brenner DJ, Krieg NR, Staley JT & Garrity GM, eds), p. 988. Springer, New York.
- Lane DJ (1991) 16S/23S rRNA sequencing. *Nucleic Acid Techniques in Bacterial Systematics* (Stackebrandt E & Goodfellow M, eds), pp. 115–175. Wiley and Sons, New York.
- Lensky NG, Dvorkin Y, Lyakhovskiy V, Gertman I & Gavrieli I (2005) Water, salt, and energy balances of the Dead Sea. *Water Resour Res* **41**: W12418.
- Machel Hans G, Krouse Roy H & Roger S (1995) Products and distinguishing criteria of bacterial and thermochemical sulfate reduction. *Appl Geochem* **10**: 373–389.
- Mukhopadhyay A, He Z, Alm EJ et al. (2006) Salt stress in *Desulfovibrio vulgaris* Hildenborough: an integrated genomics approach. *J Bacteriol* **188**: 4068–4078.
- Niggemann J, Ferdelman TG, Lomstein BA, Kallmeyer J & Schubert CJ (2007) How depositional conditions control input, composition, and degradation of organic matter in sediments from the Chilean coastal upwelling region. *Geochim Cosmochim Acta* **71**: 1513–1527.
- Nishri A & Ben-Yaakov S (1990) Solubility of oxygen in the Dead Sea brine. *Hydrobiologia* **197**: 99–104.
- Nissenbaum A (1975) The microbiology and biogeochemistry of the Dead Sea. *Microb Ecol* **2**: 139–161.
- Oren A (1983) Population dynamics of halobacteria in the Dead Sea water column. *Limnol Oceanogr* **28**: 1094–1103.
- Oren A (1988) Anaerobic degradation of organic compounds at high salt concentrations. *Antonie Van Leeuwenhoek* **54**: 267–277.
- Oren A (1999) Bioenergetic aspects of halophilism. *Microbiol Mol Biol Rev* **63**: 334–348.
- Oren A (2010) The dying Dead Sea: the microbiology of an increasingly extreme environment. *Lakes Reserv Res Manage* **15**: 215–222.
- Oren A (2011) Thermodynamic limits to microbial life at high salt concentrations. *Environ Microbiol* **13**: 1908–1923.
- Oren A (2013) Life in magnesium- and calcium-rich hypersaline environments: salt stress by chaotropic ions. *Polyextremophiles* (Seckbach J, Oren A & Stan-Lotter H, eds), pp. 215–232. Springer, Dordrecht.
- Oren A & Shilo M (1982) Population dynamics of *Dunaliella parva* in the Dead Sea. *Limnol Oceanogr* **27**: 201–211.
- Oren A & Shilo M (1985) Factors determining the development of algal and bacterial blooms in the Dead Sea:

- a study of simulation experiments in outdoor ponds. *FEMS Microbiol Lett* **31**: 229–237.
- Oren A, Gurevich P, Anati DA, Barkan E & Luz B (1995) A bloom of *Dunaliella parva* in the Dead Sea in 1992: biological and biogeochemical aspects. *Hydrobiologia* **297**: 173–185.
- Porter D, Roychoudhury AN & Cowan D (2007) Dissimilatory sulfate reduction in hypersaline coastal pans: Activity across a salinity gradient. *Geochim Cosmochim Acta* **71**: 5102–5116.
- Revsbech NP & Jørgensen BB (1986) Microelectrodes: their use in microbial ecology. *Adv Microb Ecol* **9**: 293–352.
- Revsbech NP & Ward DM (1983) Oxygen microelectrode that is insensitive to medium chemical composition: use in an acid microbial mat dominated by *Cyanidium caldarium*. *Appl Environ Microbiol* **45**: 755–759.
- Roychoudhury AN, Viollier E & Van Cappellen P (1998) A plug flow-through reactor for studying biogeochemical reactions in undisturbed aquatic sediments. *Appl Geochem* **13**: 269–280.
- Roychoudhury AN, Cowan D, Porter D & Valverde A (2013) Dissimilatory sulphate reduction in hypersaline coastal pans: an integrated microbiological and geochemical study. *Geobiology* **11**: 224–233.
- Schubert CJ, Ferdelman TG & Strotmann B (2000) Organic matter composition and sulfate reduction rates in sediments off Chile. *Org Geochem* **31**: 351–361.
- Sim MS, Bosak T & Ono S (2011) Large sulfur isotope fractionation does not require disproportionation. *Science* **333**: 74–77.
- Sorokin DY, Tourova TP, Lysenko AM & Muyzer G (2006) Diversity of culturable halophilic sulfur-oxidizing bacteria in hypersaline habitats. *Microbiology* **152**: 3013–3023.
- Spring S & Rosenzweig F (2006) The genera *Desulfotobacterium* and *Desulfosporosinus*: taxonomy. *The Prokaryotes* (Dworkin M, Falkow S, Rosenberg E, Schleifer KH & Stackebrandt E, eds), pp. 771–786. Springer, Singapore.
- Steinhorn I, Assaf G, Gat JR *et al.* (1979) Dead Sea – Deepening of the mixolimnion signifies the overture to overturn of the water column. *Science* **206**: 55–57.
- Weber M, Faerber P, Meyer V, Lott C, Eickert G, Fabricius KE & De Beer D (2007) *In situ* applications of a new diver-operated motorized microsensors profiler. *Environ Sci Technol* **41**: 6210–6215.
- Webster IT, Norquay SJ, Ross FC & Wooding RA (1996) Solute exchange by convection within estuarine sediments. *Estuar Coast Shelf Sci* **42**: 171–183.
- Wenzhöfer F, Holby O, Glud RN, Nielsen HK & Gundersen JK (2000) *In situ* microsensors studies of a shallow water hydrothermal vent at Milos, Greece. *Mar Chem* **69**: 43–54.
- Wenzhöfer F & Glud RN (2002) Benthic carbon mineralization in the Atlantic: a synthesis based on *in situ* data from the last decade. *Deep Sea Res Part I Oceanogr Res Pap* **49**: 1255–1279.
- Wieland A & Köhl M (2000) Short-term temperature effects on oxygen and sulfide cycling in a hypersaline cyanobacterial mat (Solar Lake, Egypt). *Mar Ecol Prog Ser* **196**: 87–102.

## Supporting Information

Additional Supporting Information may be found in the online version of this article:

**Fig. S1.** Map of the Dead Sea showing a close up on the sampling area.

**Fig. S2.** Rescaled microsensors profiles from Fig. 4 obtained in the WhMat1 showing the modeled (dashed line) sulfide and oxygen profiles.

**Fig. S3.** Number of specific compounds detected in the Aquifer-, spring- and the Dead Sea water.

**Fig. S4.** Salinity sensor profiles measured subsequently with the low range salinity sensor in the WhMat1 microbial mat.